Tellus (2006), 58A, 355–367
Printed in Singapore. All rights reserved

TELLUS

Numerical simulations of a severe rainfall event over the Eastern Cape coast of South Africa: sensitivity to sea surface temperature and topography

By A. T. SINGLETON and C. J. C. REASON*, *Oceanography Department, University of Cape Town, South Africa*

(Manuscript received 2 March 2005; in final form 9 Jaunary 2006)

ABSTRACT

The intense precipitation event over East London, South Africa, on 15–16 August 2002 is investigated using a mesoscale model (MM5) and its sensitivity to sea surface temperature (SST) and topography tested. Over 300 mm of rain fell in 24 h over East London as compared to the August average of 78 mm. The intense precipitation resulted from a cut-off low system aloft and the formation of a low-level jet (LLJ) near the surface.

The MM5 control simulation indicated that the intense precipitation was due to the ascent of moist air at the leading edge of the LLJ, which advected warm moist air at low levels onto the coastal mountains and was enhanced by the formation of a meso-beta scale low-pressure system just off the coast. The ascent at the leading edge of the LLJ formed the ascending arm of a convective circulation cell.

Sensitivity experiments with MM5 indicated that the warm core of the Agulhas Current contributed to the formation of the meso-beta scale low, while the mesoscale structure of the SST field was important in determining its location and that of the LLJ, and therefore the precipitation in the model. Most of the moisture originated from the Agulhas Current region. The South African topography was found to influence the location of the LLJ via trapping a near-surface warm trough on the eastern side of the Drakensberg mountains. We suggest that deficiencies in the control experiment may have been due to inaccuracies in using a weekly mean SST field to force the model at the lower boundary.

1. Introduction

A severe rainfall event affected East London on the Eastern Cape coast of South Africa in August 2002, with 24 h accumulated rainfall exceeding 300 mm—the August average is 78 mm. The heaviest rain fell around midnight 15 August local time (UTC + 2 h), with an intensity of about 85 mm h^{-1}. Several other areas along this coast also experienced heavy rainfall but not as intense as at East London, and this led to closure of its busy harbour. As shown below, the severe rainfall occurred in association with a cut-off low-pressure system at mid-levels over the western interior of South Africa. Other flood events over southern South Africa have also resulted from cut-off lows (Haywood and van den Berg, 1968, 1970; Estie, 1981; Triegaardt et al., 1988).

Cut-off lows tend to form when a trough of cold, high latitude air in the middle–upper troposphere becomes cut-off from its source region (Palmén and Newton, 1969). They are identifiable on upper air analysis charts as closed contours in the geopotential height with a warm pool found in the stratosphere above the low centre, and a cold pool found below this centre in the troposphere. Kleinschmidt (1950a,b) suggested that cut-off lows are formed by an intrusion of polar stratospheric, high potential vorticity air into the upper troposphere, and Hoskins et al. (1985) showed that cut-off lows may be identified by isolated pools of high potential vorticity air on isentropic surfaces in the mid – upper troposphere accompanied by a lowering of the dynamic tropopause.

Although most previous flood events over southern South Africa have resulted from cut-off lows, it is not understood how these systems can interact with the very strong topographic and sea surface temperature (SST) gradients of the region to locally produce very intense rainfall, or why some events produce much greater totals than others. To help address these issues, this study performs various sensitivity tests on a mesoscale model (MM5) simulation of the August 2002 event in which the SST and topography are changed.

Previous work (Taljaard, 1985) suggested that cut-off low events leading to extreme rainfall over the South African coast are often characterized by strong onshore winds advecting moist air onto the coastal mountains. South Africa is characterized by a high interior plateau of 1–2 km and steep topography at,

*Corresponding author.
e-mail: cjr@egs.uct.ac.za
DOI: 10.1111/j.1600-0870.2006.00180.x

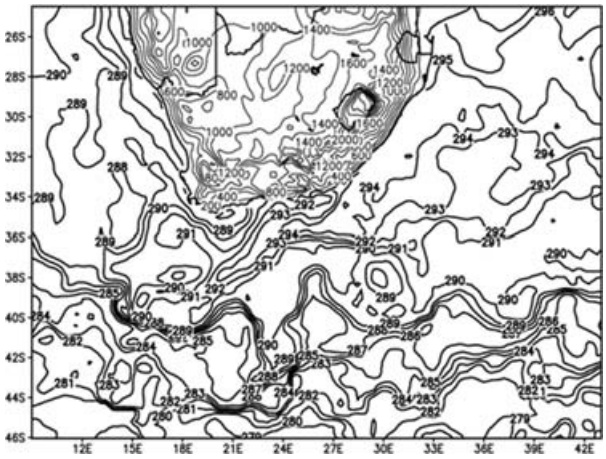

Fig. 1. Topography of South Africa from the 2 min USGS data set used to initialize MM5 (thin contours, interval 200 m), and average SST for the week of August 2002 16 from 18 km resolution NAVOCEANO data (thick contours, interval 1 K).

or near, the coast (Fig. 1), leading to strong topographic gradients and a variety of topographically forced weather systems. There are also strong SST gradients which result from coastal upwelling along the west and south coasts and the presence of the strongest western boundary current in the Southern Hemisphere, the warm Agulhas Current, along the eastern seaboard. South of South Africa, this current retroflects back into the South Indian Ocean as the Agulhas Return Current. Observational and modelling work (e.g. Walker, 1990; Jury et al., 1993; Mason, 1995; Reason and Mulenga, 1999; Reason, 2001) has demonstrated a relationship between SST in the Agulhas Current region and atmospheric circulation/rainfall over South Africa. In addition, the Agulhas Current has been suggested to act as a major source of moisture for severe rainfall events over South Africa (Crimp and Mason, 1999; Rouault et al., 2002).

The objective of this paper is to simulate the severe rainfall event of 15–16 August 2002 using the MM5 mesoscale model in order to identify the factors contributing to the rainfall, and to assess the sensitivity of the model to the SST in the Agulhas Current region, and the topography of South Africa.

A description of the synoptic evolution of the event is presented in section 2. In section 3, the model used for the numerical experiments is briefly described. Section 4 describes the results of the control experiment, with the results of the sensitivity experiments presented in section 5 and the conclusions in section 6.

2. Synoptic evolution

Analyses from the $1^\circ \times 1^\circ$ resolution National Center for Environmental Prediction (NCEP) Medium Range Forecast (MRF) model initialization fields at 12 h intervals are used to examine the evolution of the event. These fields were found to be consistent with South African Weather Service (SAWS) surface and 500 hPa synoptic charts for the period. At 0000 UTC 15 August, a day prior to the intense precipitation over East London, a cyclone existed at 500 hPa over the west of South Africa, centred near 31°S, 20°E (Fig. 2a). This feature was embedded in a cold trough slanted to the northwest with a cold pool present just south of the closed geopotential contour, and a second cold pool apparent over the ocean at 46°S, 22°E. Associated with the trough was a strong northwesterly jet flowing toward the South West Indian Ocean, while a warm ridge was present over Madagascar.

At 925 hPa, a ridge of high pressure existed south of South Africa (Fig. 3a), as is typical for cut-off low events over South Africa (Taljaard, 1985). Southeasterly onshore flow advected cold air from relatively high latitudes onto the Eastern Cape coast. Ahead of the ridge, an easterly trough advected warm, moist tropical air down the eastern seaboard of South Africa and, thus, strong low-level temperature and moisture gradients existed near the coast.

By 1200 UTC 15 August, light precipitation had begun over the Eastern Cape coast, and the mid-level cyclone had moved slightly east (centred near 31°S, 22.5°E) with strengthened cyclonic flow, and a northwesterly jet streak to the east (Fig. 2b). However, the cold pool associated with the cyclone appeared to be weaker than 12 h earlier. A stronger cold pool existed at 700 hPa (not shown) approximately co-located with the cyclone at 500 hPa, suggesting that the centre of the cut-off low had penetrated lower into the troposphere.

Near the surface (Fig. 3b), the ridge over the ocean had extended further east, while the warm trough had extended further south over the South West Indian Ocean. As a result, the onshore flow strengthened leading to the formation of an onshore low-level jet (LLJ) incident on the coast near 25.5°–27°E. The flow near the entrance region of the LLJ had become more easterly suggesting that warmer, moister, lower latitude air than earlier was being advected onto the Eastern Cape coast.

Twelve hours later (0000 UTC 16 August), when the rainfall over East London was heaviest, the trough at 500 hPa had steepened at both its apex and its bottom with a closed geopotential height contour near 32°S, 24°E and a cold pool to its southwest (Fig. 2c). A second cold pool had developed off the Namibian coast, while the northwesterly jet streak narrowed across South Africa and over the east coast, although now the maximum winds were located towards the apex of the trough over Namibia. Slowing of the winds over the Eastern Cape coast led to mid-level convergence (not shown) and facilitated lower and mid-tropospheric uplift consistent with the heavy rainfall.

At low levels (Fig. 3c), the high pressure ridged further to the east, and the warm trough east of South Africa extended further south, as the upper level jet streak narrowed. The resulting enhanced pressure gradient led to a further strengthening of the onshore LLJ whose location remained the same (Fig. 3b). The flow entering the LLJ was northeasterly, suggesting that warm, moist tropical air was being advected by the jet onto the Eastern

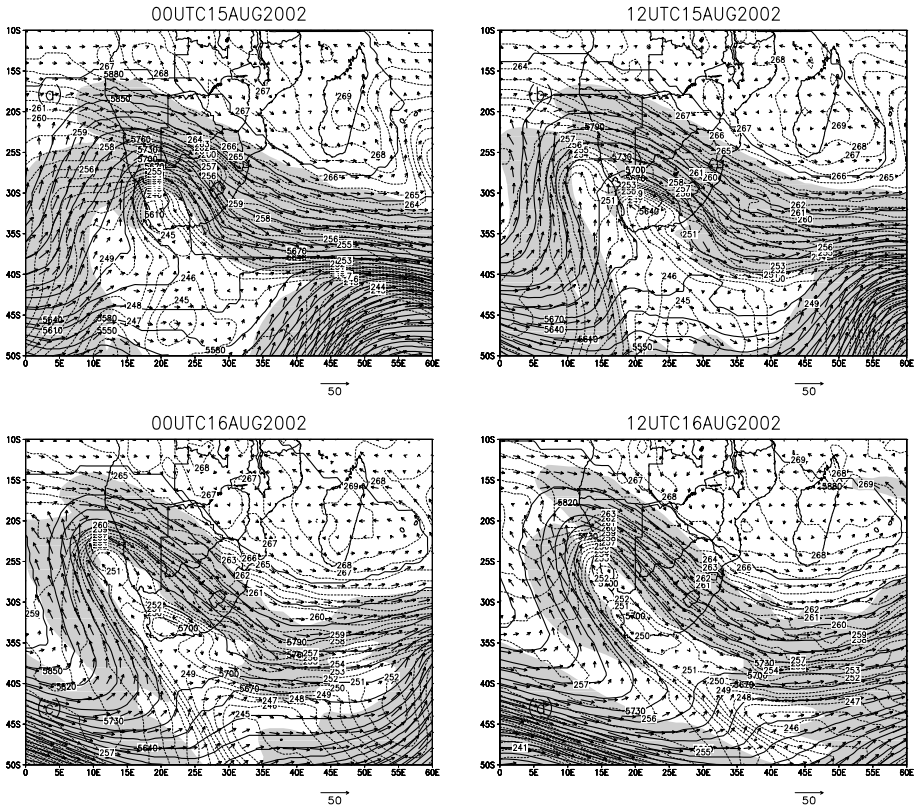

Fig. 2. MRF model analyses at 500 hPa of geopotential height (solid thick contours, interval 30 m), temperature (stippled contours, interval 1K), wind speed vectors (with a vector scale in m s^{-1} given to the bottom right of the panels), and wind speed greater than 15 m s^{-1} shaded, at 12 h intervals from (a) 0000 UTC 15 August 2002 to (d) 1200 UTC 16 August.

Cape coast where it slowed leading to low-level convergence and uplift (not shown). Infrared satellite images (not shown) revealed a large area of cloud over the Eastern Cape coast extending eastwards and approximately co-located with the LLJ, suggesting an association between this jet and the precipitation. Radiosonde data from nearby Port Elizabeth (the closest radiosonde station) showed the atmosphere to be characterized by a deep layer of nearly saturated air, with evidence of a lowered tropopause at 300 hPa (not shown).

The rainfall rate reduced over the Eastern Cape by 1200 UTC 16 August and the zonal extent of the trough at 500 hPa contracted. A second closed height contour formed towards the apex of the trough (26°S, 16°E) associated with the cold pool there (Fig. 2d). The cold pool remained near 33°S, 20°E, with a closed height contour to its north (30°S, 20°E), but there was little evidence of closed cyclonic flow. Near the surface, the ridge south of the country weakened, and the trough moved east leading to a reduced pressure gradient and vanishing of the LLJ (Fig. 3d).

The above discussion suggests that the heavy precipitation that occurred around 0000 UTC 16 August was associated with the narrowing of the upper level jet streak, low and mid-level convergence, accompanied by a steepening near-surface pressure gradient resulting in strong onshore flow. The synoptic influence of upper level jet streaks on surface flow involves surface convergence on the poleward side of upper level jet streak exit regions (Barry and Chorley, 1992) indicating that East London should be the area which received the most heavy rainfall as it is located just polewards of the upper level jet exit near 32°S. In addition, the cold upper-air trough contributed to the instability in the region.

Consideration of the synoptic forcing alone cannot explain the extreme rainfall observed over a relatively small coastal area. Therefore, the modelling study that follows investigates the influence of the surface forcing in the presence of a cut-off low-pressure system aloft.

3. Model description and data

The model used in this study is version 3 of the fifth generation of the Pennsylvania State University – National Center for Atmospheric Research Mesoscale Model, MM5 (Grell et al., 1994). This non-hydrostatic model has been used with some success in simulating extreme precipitation events in many parts of the Northern Hemisphere (e.g. Colle and Mass, 2000; Romero et al., 2000; Yeh and Chen, 2002). However, there is little evidence in the literature that MM5 has been widely applied to Southern

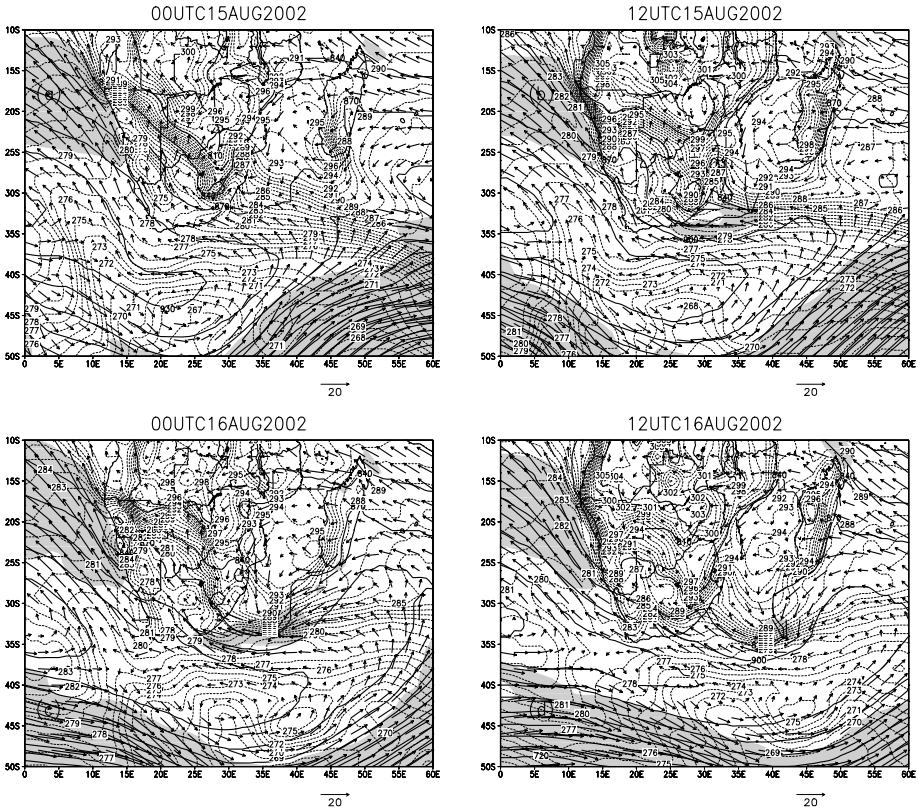

Fig. 3. As in Fig. 2 except at 925 hPa and wind speed greater than 15 m s^{-1} shaded.

Hemisphere extreme weather events. Given the different land–sea distributions in the Southern Hemisphere, and the unique proximity of one of the world's strongest warm western boundary currents (Agulhas) to an intense coastal upwelling system (Benguela) in a region of strong topographic gradients (southern South Africa), it is of interest to study how well MM5 can represent an extreme weather event in this different setting.

In this study, a horizontal resolution of 27 km was initially used on a single grid of 142 × 112 grid points centred at 36°S, 26°E. In the vertical, 40 σ levels were used, with increased resolution in the lowest kilometre in order to adequately resolve the boundary layer. Topography was taken from the USGS 5-min resolution data set and interpolated onto the model grid using a Cressman type objective analysis scheme (Cressman, 1959).

Initial and boundary conditions (atmospheric variables, and soil moisture and temperature) were interpolated from the 1° × 1° resolution MRF model onto the MM5 grid. Initial imbalances of these fields were reduced by iteratively removing the vertical integral of the horizontal divergence at each grid point (Grell et al., 1994). Boundary conditions were imposed every 12 h (higher temporal resolution data were not available to us).

The 18 km weekly interpolated Advanced Very High Resolution Radiometer (AVHRR) SST product of the National Oceanographic Office (NAVOCEANO), held constant throughout the simulation, was used to force the model. Boundary layer processes were parametrized using the MRF scheme (Hong and Pan, 1996) while surface land temperature and moisture were calculated using the Noah land-surface model (Chen and Dudhia, 2001a,b), which considers soil properties up to 4 m below the surface. The calculation of longwave and shortwave radiative effects on atmospheric temperature tendencies and surface fluxes included the effects of cloud cover. Moist convection was parametrized using Grell (1993). The explicit microphysics parametrization, which uses predictive equations for cloud water and rain water below the freezing level and cloud ice and snow above the freezing level, was employed. The effects of evaporation, condensation, hydrostatic water loading, melting, freezing, deposition, sublimation and supercooled liquid water are all included in this scheme.

4. Control simulation (CNTRL experiment)

In this section, the results of CNTRL with full physics and high resolution SST are compared with MRF model analyses and available observational and satellite data. Figure 4 shows the observed and CNTRL 24 h precipitation valid at 0700 UTC 16 August. Although the relative paucity of rainfall stations prevents a detailed comparison, Fig. 4 gives some indication of

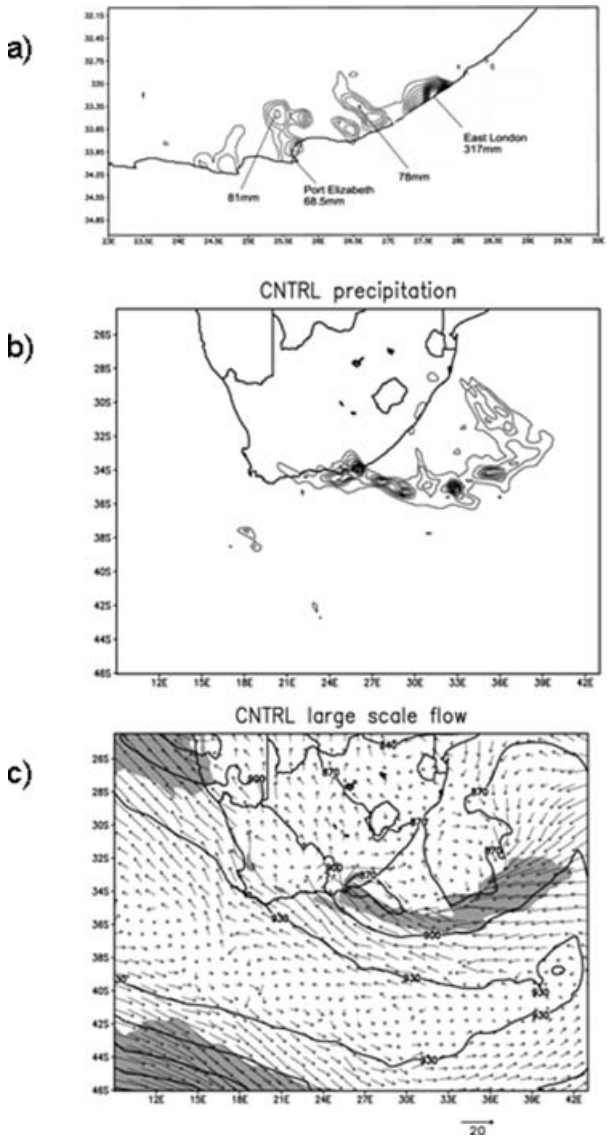

Fig. 4. (a) Objectively analysed observed rainfall from SAWS rain gauges for the 24 h period to 0700 UTC 16 August 2002 (contour interval 20 mm); (b) Precipitation from CNTRL for the 24 h period to 0700 UTC 16 August (contour interval 20 mm); and (c) 925 hPa geopotential height (solid contours, interval 30 m), temperature (stippled contours, interval 1K), wind vectors (with a scale vector in m s^{-1} given to the bottom right of the panels) and wind speed greater than 15 m s^{-1} shaded at 0000 UTC 16 August 2002 from CNTRL

the model performance for precipitation. The recorded rainfall at East London (33°S, 27.5°E) was 317 mm (Fig. 4a) whereas CNTRL simulated a maximum of 190 mm just off the coast at 34°S, 26°E (Fig. 4b). However, it was found (not shown) that the timing of the most intense precipitation in CNTRL compared well with that observed, suggesting that the precipitation maximum in the model corresponds to the maximum observed at East London. In addition, comparison of time series of surface pressure and air temperature from eight South African Weather Service automatic weather stations in the Eastern Cape with output from CNTRL (not shown) indicates that the model timing of the largest changes in pressure and temperature as well as their tendencies are consistent with the observed. Over the ocean, CNTRL shows a zonal band of precipitation east of the Eastern Cape, co-located with the cloud observed in the corresponding satellite image (not shown), and also reflected in the Tropical Rainfall Measuring Mission (TRMM) rainfall (not shown).

Comparing Fig. 3c with Fig. 4c suggests that CNTRL did not adequately resolve the position of the onshore LLJ since it shows the jet impinging on the Eastern Cape coast about 150 km west of the MRF analysis. However, many other aspects of the large-scale flow were adequately resolved in CNTRL, suggesting that its main deficiency was in correctly simulating the area of the extreme precipitation. Further experiments were undertaken with different parametrizations for boundary layer processes and sub-gridscale convection, but the choice described in section 3 produced the results that best compare with the MRF analyses. The model was also re-run with two nested grids centred over East London using two-way nesting at 9 km and 3 km resolution, with 2 min and 30 s topography. There was little improvement in the LLJ location or precipitation maxima with the enhanced resolution, so the massive increase in computational expense of sensitivity studies using two nested grids was not justified.

CNTRL compared very favourably with the MRF analysis at mid-levels as well as with South African Weather Service surface and 500 hPa synoptic charts suggesting that the MM5 inaccuracies in the location of the LLJ and precipitation maximum were due to problems in adequately simulating processes in the lower troposphere. Therefore, we believe that it is possible to draw some tentative conclusions about the event based on the 27 km resolution run, and to investigate the sensitivity of the model to the topography and complex SST forcing. Thus, only simulations undertaken with a single 27 km resolution grid are discussed below. It should be emphasized that we consider CNTRL as a reference case against which we compare the results from the various sensitivity experiments discussed below.

4.1. Mesoscale aspects

The reference time of 0000 UTC 16 August 2002 is chosen since this is when the heaviest rainfall occurred in both the observations and CNTRL. One of the most striking aspects of the large-scale flow in CNTRL at this time (Fig. 4c) was the formation of a meso-beta scale low-pressure system off the Eastern Cape coast near 26°–27.5°E and stronger low-level pressure gradients over the coastal ocean. Relatively weak cyclonic flow is evident to the north of the LLJ near 31°S, 33°E in the MRF field (Fig. 3c) as well as in the morning pass of the QuikSCAT scatterometer for this day, that is, further east than in CNTRL, consistent with the shift in the precipitation maximum and the LLJ in CNTRL.

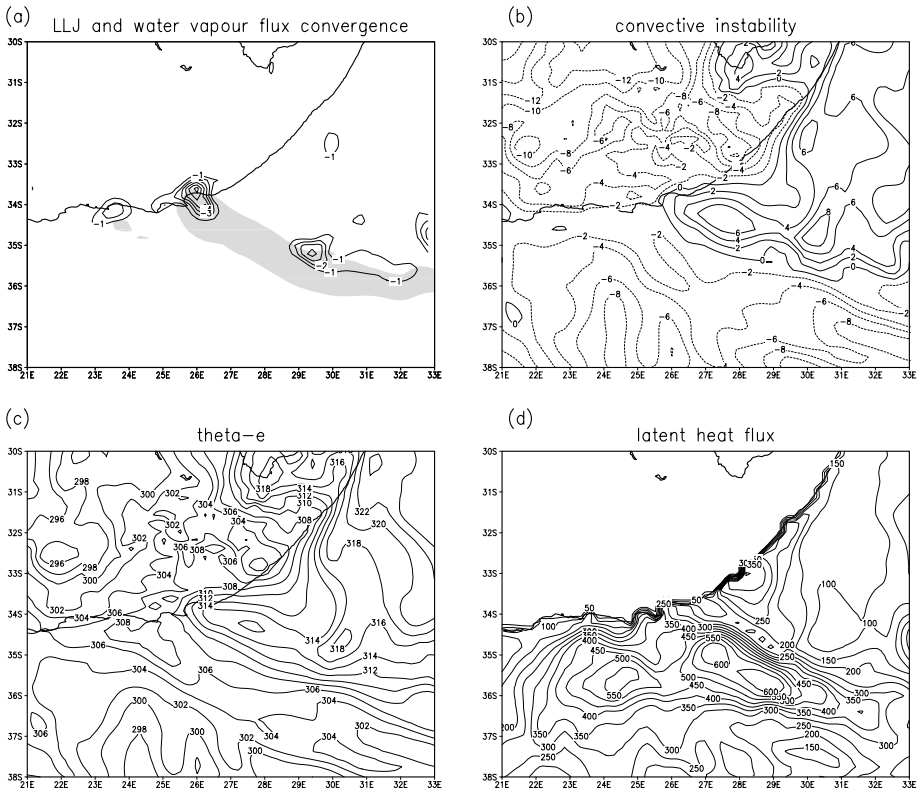

Fig. 5. Output from CNTRL at 0000 UTC 16 August 2002. (a) 1000–850 hPa water vapour flux convergence, contour interval 1 g m^{-2} s^{-1}, with wind speed greater than 15 m s^{-1} shaded; (b) Convective instability taken as the difference in equivalent potential temperature between 1000- and 500-hPa, contour interval 5K; (c) 1000 hPa equivalent potential temperature, contour interval 2K; (d) surface latent heat flux, contour interval 50 W m^{-2}.

Although it might seem logical to suggest that the meso-beta scale low formed as a result of lee troughing as the mid-level northwesterly flow interacted with the Drakensberg mountains of eastern South Africa, this low was present in a simulation with the topography removed. Animated sequences of the flow pattern show that the meso-low formed about 200 km southeast of its location in Fig. 4c at around 0500 UTC 15 August as the cool air of the upper trough approached this region, and enhanced the instability. Shortly thereafter, heavy precipitation began on the poleward side of this meso-low. The subsequent movement of the meso-low towards the coast was approximately in phase with the propagation of the heaviest precipitation. This sequence of events suggests that the meso-low most likely formed as a result of destabilization of the atmosphere due to the advection of cold air aloft and then moved towards and off the coast and intensified due to latent heat release in the atmospheric column over the heavy precipitation. Once over the coastal ocean, surface heating over the warm waters of the Agulhas Current enhanced the instability further. An examination of the temperature evolution in the mid-levels of the atmosphere during this time (not shown) supports the hypothesis that latent heat release influenced the movement of the meso-low as a warm core air-mass moved approximately in phase with the system.

The meso-beta scale low appeared to provide additional forcing to the LLJ, increasing the onshore wind speed. The LLJ was characterized by strong horizontal wind shear on its right-hand flank and strong low-level water vapour flux convergence, the latter was greatest where the jet impinged on the coast (Fig. 5a). An area of convectively unstable stratification existed over the coastal ocean east of 25.5°E, and this just penetrated onto the land near East London (Fig. 5b). This instability arose from warm, moist air extending down the east coast towards East London with a tongue of high θ_e air present between 26°E and 30°E (Fig. 5c). Thus, the extreme rainfall during this event was the result of warm moist air being advected onto the Eastern Cape coast of South Africa where vigorous ascent occurred due to large low-level water vapour flux convergence at the coastal mountains. There were also large surface latent heat fluxes (500–600 W m^{-2}) from the ocean in the LLJ region (Fig. 5d), indicating that the warm SST of the Agulhas Current contributed to the low-level moisture supplying the rainfall.

A cross-section along the axis of the LLJ where it impinged on the coast shows that there was strong ascent near the coast, forming the upward branch of a convective cell with a weaker descending branch to the southeast (Fig. 6), as well as farther offshore (not shown). Examining cross-sections at other times

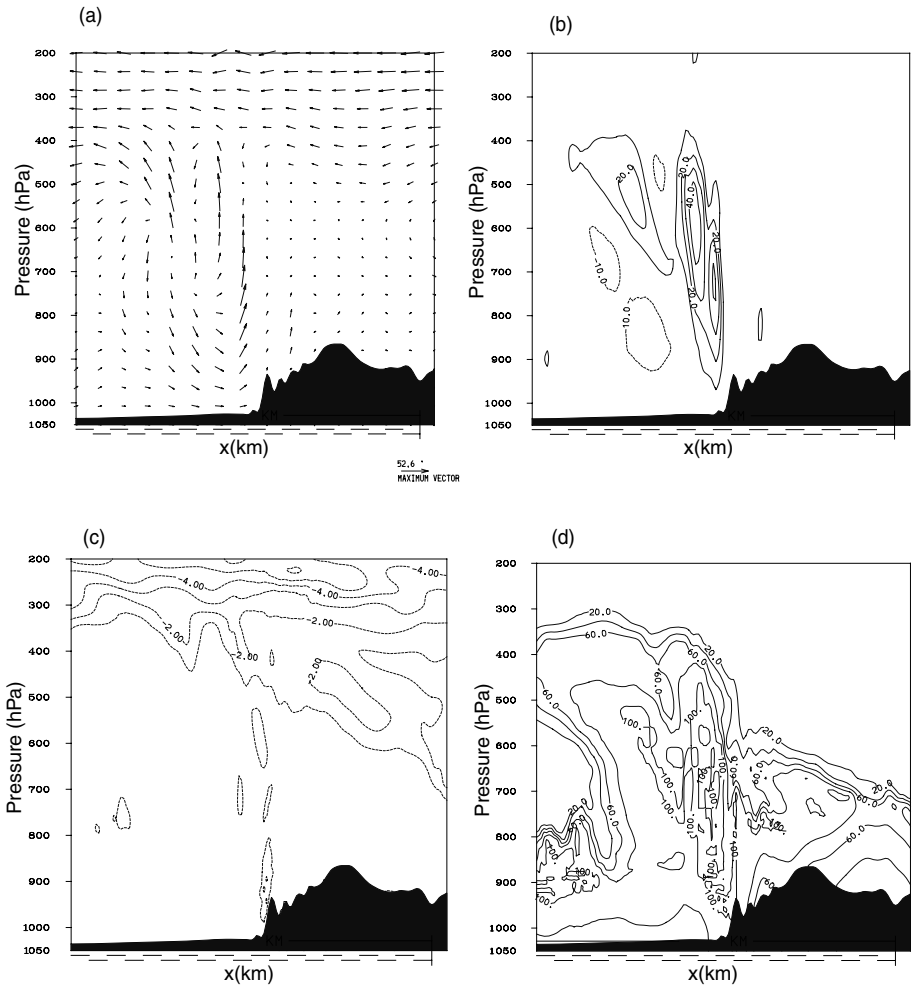

Fig. 6. Cross-section along the axis of the low-level jet from CNTRL at 0000 UTC 16 August 2002 showing (a) wind vectors in the plane of the cross-section, (b) vertical velocity (contour interval 10 cms^{-1}), (c) potential vorticity (contour interval 1 PVU); and (d) relative humidity (contour interval 20%). The horizontal axis extends 2000 km in each case (1000 km off the coastline and 1000 km inland).

(not shown) indicated that this convective cell was initially located over the ocean and approached the coast from the southeast in phase with the meso-low. As it reached the south coast, the ascending arm was strengthened considerably, with upward velocities close to 50 cm s^{-1} (Fig. 6b), rather large for a simulation with this spatial resolution. This result suggests that the coastal topography played a role in enhancing the ascending branch of the convective cell, which is discussed further in section 5. The potential vorticity (Fig. 6c) shows a tropopause fold towards the northwest above the interior South African plateau, suggesting an intrusion of cold stratospheric air into the troposphere potentially strengthening the instability. In addition, a plume of high potential vorticity air from the coastal mountain peak up to the tropopause was present (Fig. 6c). Since potential vorticity is conserved in adiabatic conditions (Hoskins et al., 1985), the generation of potential vorticity in the lower troposphere suggests that some diabatic process was taking place. In this convective environment, it is likely that latent heat release due to condensation was responsible since Fig. 6 shows that the potential vorticity plume is co-located with the vigorous ascent that took place in an almost fully saturated environment (Fig. 6d).

In summary, a warm moist LLJ, enhanced by a meso-beta scale low, advected warm moist air onto the Eastern Cape coast of South Africa. Convection was associated with convergent flow on the right-hand edge of the LLJ and a convective cell with its ascending branch at the leading edge of the LLJ. When the LLJ impinged on the south coast, the vertical velocity in the ascending branch of the convective cell was strengthened. High latent heat flux values over the ocean suggest that the warm SST of the Agulhas Current contributed low-level moisture to the rainfall event, as well as providing sufficient heat to the boundary layer to destabilize the lower troposphere. These contributing factors are investigated in more detail in the following section through a series of sensitivity experiments.

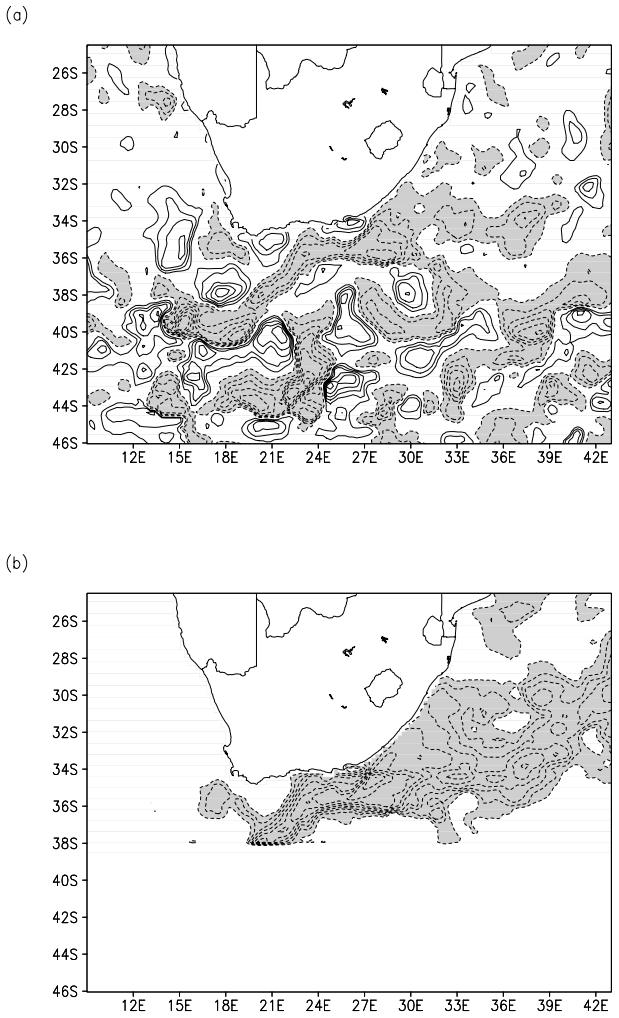

Fig. 7. Sea surface temperature anomalies corresponding to (a) the LRSST experiment, and (b) the NOAGL experiment. The contour interval is 0.5 K and cool anomalies are represented by dashed contours and shading, and warm anomalies represented by solid contours.

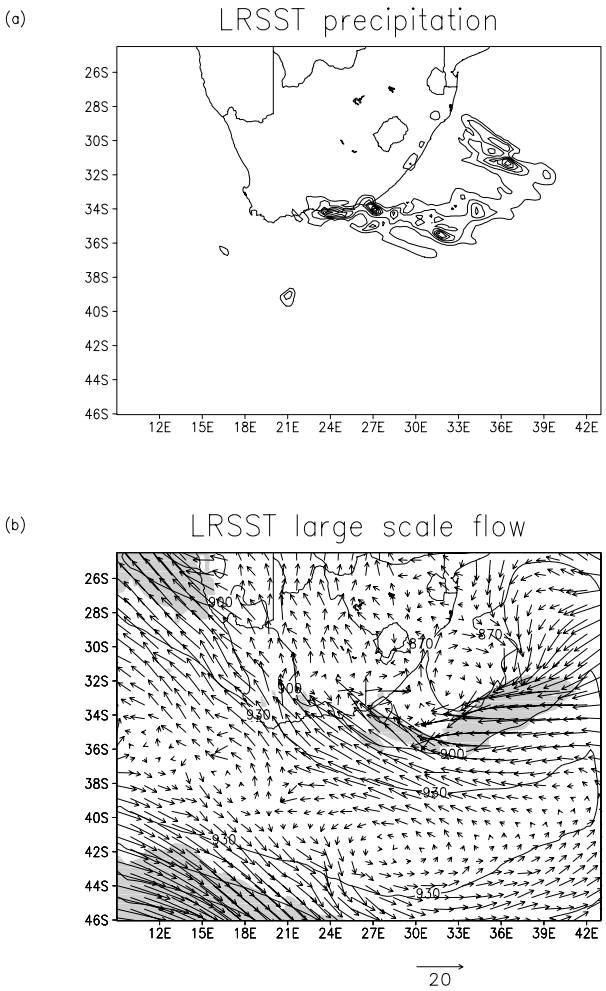

Fig. 8. (a) Precipitation from LRSST for the 24 h period to 0700 UTC 16 August (contour interval 20 mm); and (b) 925 hPa geopotential height (solid contours, interval 30 m), temperature (stippled contours, interval 1K), wind vectors (with a scale vector in m s^{-1} given to the bottom right of the panels) and wind speed greater than 15 m s^{-1} shaded at 0000 UTC 16 August 2002 from LRSST.

5. Sensitivity experiments

5.1. Sea surface temperature (LRSST and NOAGUL experiments)

Two experiments were constructed to investigate the effects of SST on this event. The first experiment, LRSST, used lower resolution (1° × 1°) SST from the Optimal Interpolation Sea Surface Temperature (OISST) data set. The difference between OISST and the 18km resolution NAVOCEANO SST is shown in Fig. 7a. OISST did not include the cold upwelling south of Port Elizabeth seen in NAVOCEANO and the core of the Agulhas Current was up to 2 K cooler. In the second experiment, NOAGL, the warm Agulhas Current was removed from the NAVOCEANO data used in CNTRL, by setting SST > 291 K south of 33°S to 291 K. This resulted in an SST anomaly shown in Fig. 7b, with the core of the Agulhas Current up to 4 K colder.

The precipitation pattern in LRSST (Fig. 8a) was broadly similar to CNTRL (Fig. 4b). However, the precipitation maximum was further southeast of the coast in LRSST and was considerably lower (143 mm), with less inland penetration of the rainfall. Further west (23°–25°E), the precipitation was higher in LRSST and penetrated further inland. These differences in the precipitation pattern were reflected in the large-scale flow for LRSST at 0000 UTC 16 August (Fig. 8b), with the meso-beta scale low situated about 1° to the east north east, and smaller in scale compared with CNTRL (Fig. 4c). This displacement supports the suggestion that the meso-low was contributed to by surface heating since it is located near 27°–28°E, 34°S where the SST is

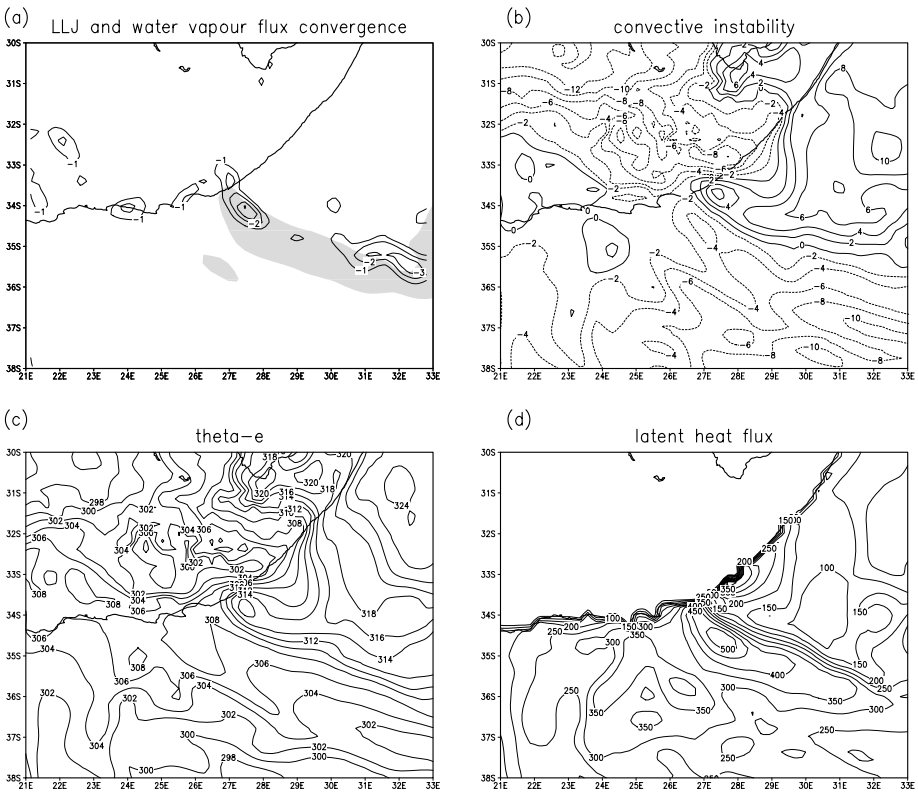

Fig. 9. As in Fig. 5 except from LRSST.

near maximum (eastern part of warm coastal anomaly in Fig. 7a and western part of Agulhas Current). As a result, the LLJ was located a similar distance to the east northeast, with less inland penetration of the onshore flow. To the west, where the rainfall was greater in LRRST, there was little appreciable difference in the large-scale flow, except that the onshore wind was slightly stronger in LRSST with slightly warmer low-level temperature, due to the lack of inshore upwelling in the SST field near 22°–25°E, 34°S (Fig. 7a).

The low-level water vapour flux convergence at the leading edge of the LLJ in LRSST (Fig. 9a) was much weaker than in CNTRL (Fig. 5a) at this time, with its maximum slightly to the south of the coast. However, the area of maximum convective instability in LRSST (Fig. 9b) was located closer to the coast than in CNTRL (Fig. 5b). This occurred because the tongue of high θ_e air, which was considerably narrower in LRSST (Fig. 9c), was closer to the land and farther to the northeast compared with CNTRL (Fig. 5c), due to the cooler SST in LRSST in this region. Surface latent heat fluxes near 27°–28°E (400–500 W m^{-2}) were also slightly lower in LRSST (Fig. 9d) compared with CNTRL (500–600 W m^{-2}) (Fig. 5d).

It therefore appears that the mesoscale SST structure south of the Eastern Cape coast, where there were large differences between the high resolution NAVOCEANO and the lower resolution OISST data sets, was important in determining the location of the LLJ, with the warmer core of the Agulhas Current in the NAVOCEANO SST field extending farther west compared with the corresponding OISST data. However, the cold upwelled SST to the south of Port Elizabeth in the CNTRL experiment appears to have had less impact on the event in this region, but may have accounted for the smaller amount of rainfall simulated in CNTRL between 23°E and 25°E than in LRSST.

In the NOAGL experiment, the effect of the warm core of the Agulhas Current was further investigated by removing it from the SST forcing field. The broad pattern of the precipitation field was similar in NOAGL (Fig. 10a) compared with CNTRL (Fig. 4b), but the amount of rainfall generated was much less, especially near the coast, where only around 20 mm was simulated. Correspondingly, the large-scale flow at the reference time (0000 UTC 16 August) showed much weaker onshore flow, with the LLJ not reaching the coast (Fig. 10b). There was no meso-beta scale low in NOAGL (Fig. 10b) and the pressure gradient forcing near the coast was much weaker. The lack of a meso-low in NOAGL indicates that surface heating due to the Agulhas Current, whose waters are up to 5 K warmer than further offshore, played a large role in the formation of this low in CNTRL by enhancing the low-level instability in the presence of cold air aloft. The offshore trough seen in CNTRL near 33°E is shifted north in NOAGL to near 30°–32°S where the SST is warmer and, as a result of the coastline orientation, is nearer the coast leading to the northern precipitation maximum seen in Fig. 10a.

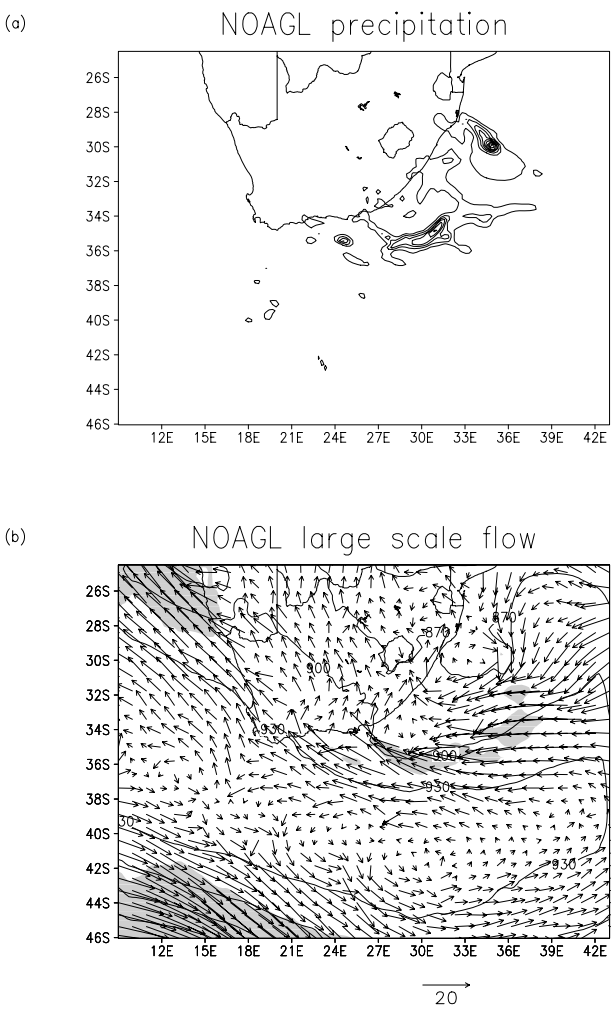

Fig. 10. As in Fig. 8 except from NOAGL.

As in CNTRL, areas of low-level water vapour flux convergence in NOAGL were associated with the right-hand and leading edges of the LLJ (Fig. 11a). However, a larger portion of the ocean south of the Eastern Cape displayed convective instability in NOAGL (Fig. 11b), but weaker than in CNTRL (Fig. 5b). There was some evidence of a tongue of relatively high θ_e air in NOAGL (Fig. 11c), which appeared to be approximately co-located with the LLJ (Fig. 11a). However, the maximum temperature of 310 K was 6 K cooler than this high θ_e tongue in CNTRL. As a result of the cooler SST, the surface latent heat flux in NOAGL (Fig. 11d) was much less than that simulated in CNTRL (Fig. 5d), indicating that there was less evaporation from the ocean and reduced low-level moisture supplied to the system.

The above suggests that removing the Agulhas Current resulted in cooler, drier air in the boundary layer leading to insufficient supply of low-level moisture and buoyancy to facilitate the occurrence of deep convection and extreme rainfall as the onshore flow reached the coast.

5.2. Topographic effects—NOTOP experiment

Topographic effects were investigated by setting the entire topography over land to zero (NOTOP). The precipitation pattern over the ocean in NOTOP (Fig. 12a) was broadly similar to that in CNTRL (Fig. 4b). However, the coastal rainfall showed no obvious peak, instead being concentrated further west between 22°E and 25°E, with a maximum around 23.5°E. The large-scale flow was characterized by the LLJ covering a much larger area all the way up western South Africa towards Namibia (Fig. 12b). The meso-beta scale low was located over the land and to the west compared with CNTRL (Fig. 4c), since the low-level trough was now situated over the whole of eastern South Africa in NOTOP. This result suggests that the 2.5–3.5-km-high Drakensberg mountains over eastern South Africa were responsible for maintaining the position of this trough off the east coast of South Africa, and thus influenced the location of the meso-beta scale low and the LLJ. The continued presence of the meso-beta scale low in NOTOP but not in NOAGL indicates that this low resulted from destabilizing of the mid- and lower troposphere due to surface heating associated with the Agulhas Current coupled with cold air advection aloft rather than from lee-trough formation—the LLJ then advected the low inland in NOTOP.

The low-level water vapour flux convergence in NOTOP was clearly associated with the circulation of the meso-beta scale low converging with the onshore flow of the LLJ near 34°S, 25°E (Fig. 13a). Convectively unstable stratification was mostly concentrated over the ocean (Fig. 13b) slightly south of the main area of convective instability in CNTRL (Fig. 5b). Although warm moist air was apparent at low levels in NOTOP (Fig. 13c), it did not form into a narrow tongue penetrating onto the coast as seen in CNTRL (Fig. 5c), and a wide tongue of dry air, not seen in CNTRL, extended over the land from the north in NOTOP (Fig. 13c). This spreading of dry air from the north likely resulted from the lack of topography now allowing the dry continental air mass that exists over South Africa in winter to mix down to the coast. The maximum surface latent heat flux in NOTOP (Fig. 13d) was as high (500–600 W m^{-2}) as in CNTRL (Fig. 5d), but was located to the west in NOTOP due to the high wind speeds of the LLJ there. The removal of the topography had a considerable effect on the large-scale flow and the location of the precipitation maximum. With no topography to block it, the LLJ was able to penetrate far inland.

6. Discussion and conclusions

A case study of a severe rainfall event over the South African southeast coast, in which about four times the monthly average rainfall for August fell over East London in just 24 h, was studied with the aid of analyses from the MRF model and numerical simulations using MM5. Over western South Africa, the MRF analyses showed that the event was characterized by

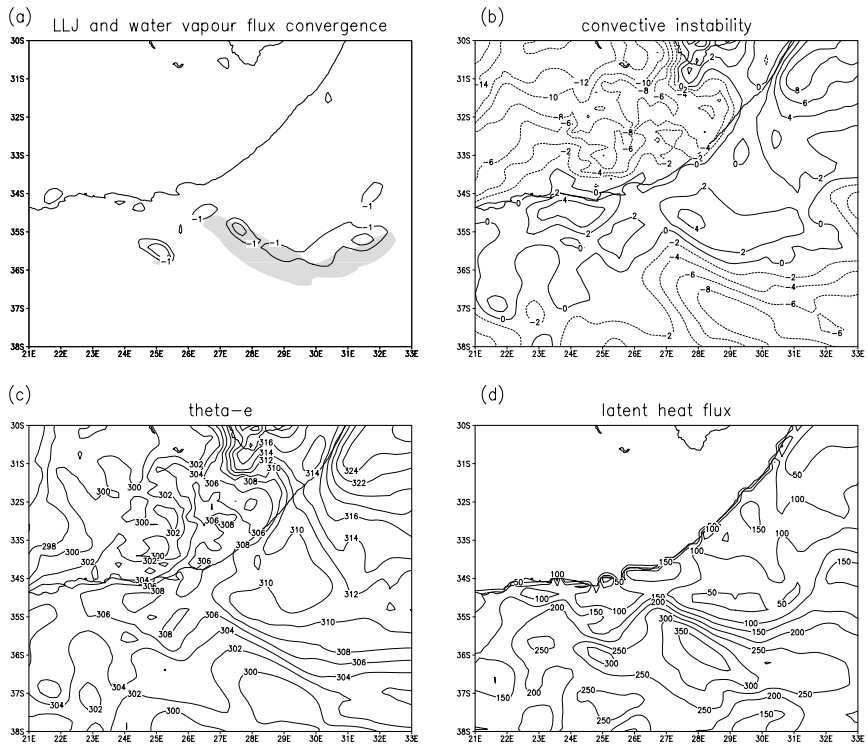

Fig. 11. As in Fig. 5 except from NOAGL.

a cut-off low-pressure system in the middle troposphere. The near surface flow was characterized by a ridge of high pressure over the ocean south of the country and a warm trough to the east, which led to the formation of a LLJ impinging onto the coast in the vicinity of the location of the heaviest rainfall.

A MM5 simulation of the event produced the severe rainfall and the LLJ about 150 km west of the MRF analysis. Since the MM5 simulation reproduced most of the salient features of the event (albeit at slightly different locations), we believe some tentative conclusions may be drawn with regard to the factors contributing to this event. MM5 suggested that a meso-beta scale low formed to the southeast of the Eastern Cape coast as cold air advection aloft coupled with the warm SST of the Agulhas Current destabilized the atmosphere. This meso-low enhanced the strength of an onshore LLJ as it moved towards the coast under the influence of latent heat release. Strong low-level convergence of moist air at the leading edge of the LLJ in the presence of convectively unstable stratification was responsible for the heavy rainfall observed over the Eastern Cape coast. The ascent of moist air at the leading edge of the LLJ, enhanced by coastal topography, formed the ascending branch of a convective cell, with evidence of a weak descending branch to the southeast. Also associated with the LLJ was a near-surface tongue of warm moist air, and high latent heat fluxes from the Agulhas Current, indicating that its warm SST influenced the event through destabilizing the boundary layer and adding low-level moisture.

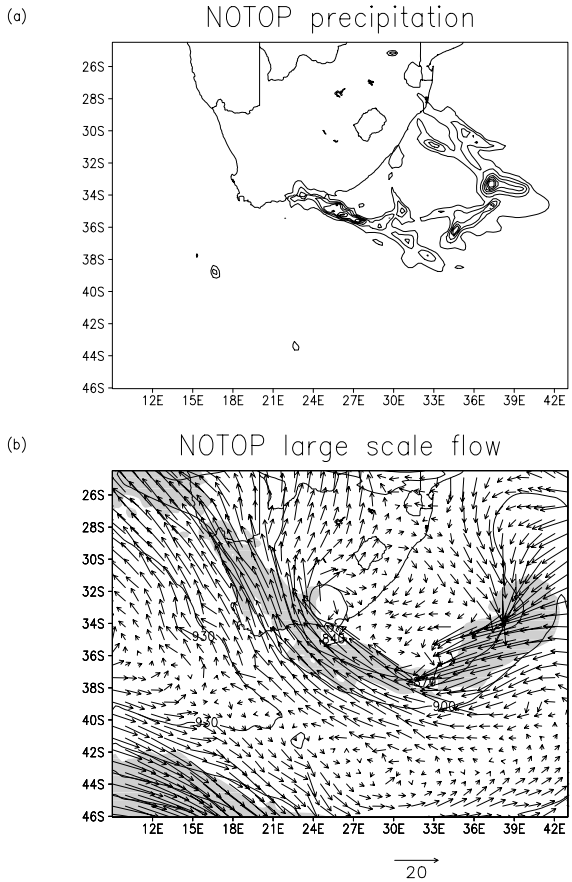

Fig. 12. As in Fig. 8 except from NOTOP.

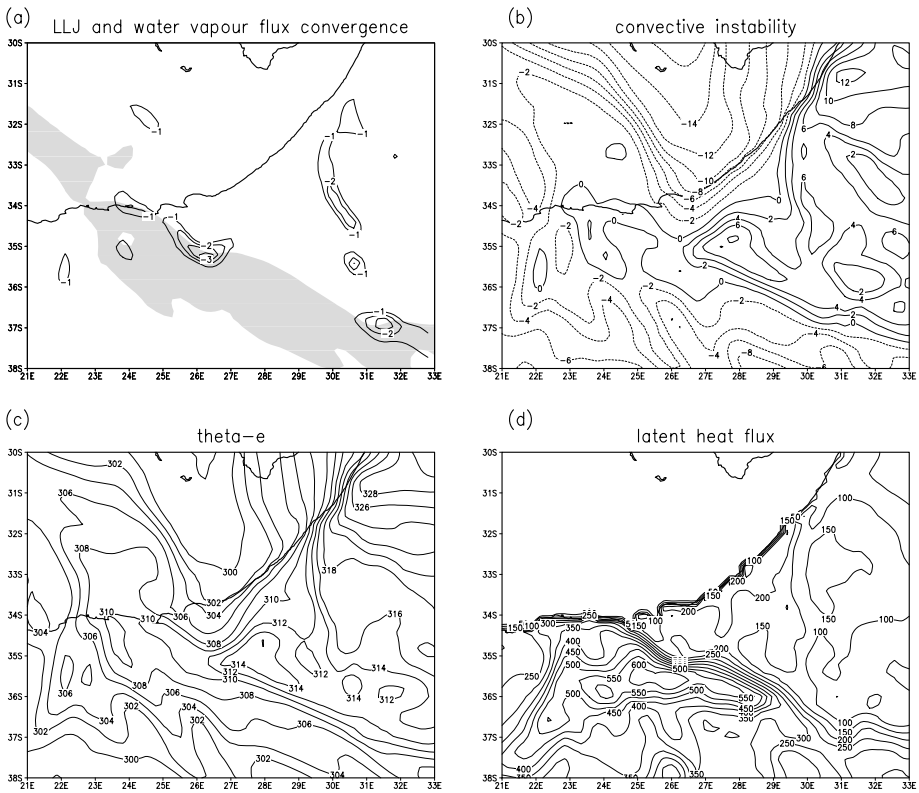

Fig. 13. As in Fig. 5 except from NOTOP.

A series of sensitivity tests with the model was undertaken to assess the contribution of physical factors (SST and topography). It was found that the topography of South Africa had a considerable effect on the location and amount of precipitation generated in the simulation. An experiment with zero topography suggested that the high topography of the Drakensberg mountain range was responsible for blocking the inland penetration of the warm trough over the ocean to the east of South Africa during the event, which led to the advection of warm, moist, tropical air over the ocean down the eastern side of the country. This in turn influenced the location of the onshore LLJ, which was blocked by the coastal topography and forced to rise leading to the heavy rainfall. In order to test whether the meso-beta low was mainly due to instability effects rather than lee troughing, a second topography experiment was done in which the coastal topography of the Eastern Cape only was removed. In this case, the meso-low extended from the Agulhas Current region about 100 km inland (not shown) consistent with it being forced mainly by heating effects plus inland advection by the LLJ rather than from lee troughing of the northwesterly mid-level flow. If lee troughing was responsible, then the meso-low would not occur during the experiment with zero topography (NOTOP). Instead, the meso-low does occur in NOTOP and extends substantially inland.

Forecast models used by the SAWS do not use SST products with as high a resolution as the 18 km of NAVOCEANO. The LRSST experiment clearly shows that reducing the resolution of the SST field to that used by forecast models, greatly affects the output in a cut-off low event. In LRSST, the region of heaviest rainfall, the meso-beta scale low and the LLJ were shifted about 1° to the east northeast relative to the CNTRL run. While this would appear to be a more accurate position for the LLJ compared with the MRF analysis, it led to further inaccuracies in the location of the maximum precipitation with very little precipitation over the land.

The mesoscale structure of the SST field and the strong SST gradients associated with the Agulhas Current and inshore upwelling appear to have had a considerable influence on the location of the rainfall, pointing to a potential weakness in the CNTRL simulation. The high resolution SST data used was a weekly interpolated mean, so day to day variability was not taken account of. Unfortunately, it is difficult to get daily satellite derived SST fields in this region since they are obscured by cloud. An alternative would be to use microwave sensor derived SST from TRMM, which is able to detect through cloud, but data within 35 km of the coast are considered unreliable.

The experiment with the Agulhas Current removed (NOAGL) showed the important influence that the warm core of the current had on this cut-off low event. The cold air aloft did not sufficiently destabilize the atmosphere for the important meso-beta scale low to form without the low-level heating from the warm SST of the Agulhas Current. In turn, the meso-low led to an

enhancement of the LLJ and convection resulting in the extreme rainfall observed.

The results of the LRSST and NOAGL experiments highlight the sensitivity of model simulations to the SST forcing in this region, where the warm Agulhas Current and coastal upwelling leads to strong SST gradients. These results suggest that it is very important for forecasting applications in South Africa that an appropriately high-resolution representation of the Agulhas Current is included in a forecast model since the location and intensity of the rainfall in these type of severe weather events may depend heavily on the SST forcing used. In addition, the results point to the need for adequate representation of local topography since the model simulation indicated that the Drakensberg/Maluti mountains helped to determine the location of the LLJ, and therefore the heavy precipitation for this cut-off low event.

7. Acknowledgments

We thank Eumetsat for providing the Meteosat images, and the South African Weather Service for precipitation data. The NAVOCEANO and OISST data were obtained from http://podaac.jpl.nasa.gov/poet at the Physical Oceanography Distributed Active Archive Center (PO.DAAC), NASA Jet Propulsion Laboratory, Pasadena, CA. K. Hansingo assisted with the figures.

References

Barry, R. G. and Chorley, R. J. 1992. *Atmosphere, Weather and Climate*, 6th Edition. Routledge, New York, 392 pp.

Chen, F. and Dudhia, J. 2001a. Coupling an advanced land-surface/hydrology model with the Penn State/NCAR MM5 modeling system. Part I: Model implementation and sensitivity. *Mon. Wea. Rev.* **129**, 569–585.

Chen, F. and J. Dudhia, 2001b. Coupling an advanced land-surface/hydrology model with the Penn State/NCAR MM5 modeling system. Part II: Preliminary model validation. *Mon. Wea. Rev.* **129**, 587–604.

Colle, B. A. and Mass, A. F. 2000. The 5–9 February 1996 flooding event over the Pacific Northwest: Sensitivity studies and evaluation of the MM5 precipitation forecast. *Mon. Wea. Rev.* **128**, 593–617.

Cressman, G. 1959. An operational analysis system. *Mon. Wea. Rev.* **87**, 367–374.

Crimp, S. J. and Mason, S. J. 1999. The extreme precipitation event of 11–16 February 1996 over South Africa. *Met. Atmos. Phys.* **70**, 29–42.

Estie, K. E. 1981. The Laingsburg flood disaster of January 1981. *South African Weather Bureau Newsletter* **383**, 19–32.

Grell, G. A. 1993. Prognostic evaluation of assumptions used by cumulus parameterizations. *Mon. Wea. Rev.* **121**, 764–787.

Grell, G. A., Dudhia, J. and Stauffer, D. R. 1994. A description of the fifth generation Penn State/NCAR mesoscale model (MM5). NCAR Tech. Note NCAR/TN-398 + STR, 122 pp.

Haywood, L. Q. and Van den Berg, H. 1968. Die Port Elizabeth storeëns van 1 September 1968. *South African Weather Bureau Newsletter* **234**, 157–169.

Haywood, L. Q. and Van den Berg, H. 1970. The Eastern Cape floods of 24–28 August 1970. *South African Weather Bureau Newsletter* **257**, 129–141.

Hong, S.-Y. and Pan, H.-L. 1996. Nonlocal boundary layer vertical diffusion in a medium-range forecast model. *Mon. Wea. Rev.* **124**, 2322–2339.

Hoskins, B. J., McIntyre, M. E. and Robertson, A. W. 1985. On the use and significance of isentropic potential vorticity maps. *Quart. J. Roy. Met. Soc.* **111**, 877–946.

Jury, M. R., Valentine, H. R. and Lutjeharms, J. R. E. 1993. Influence of the Agulhas Current on summer rainfall along the southeast coast of South Africa. *J. Appl. Meteor.* **32**, 1282–1287.

Kleinschmidt, E. 1950a. Uber aufbau und entstehung von zyklonen I. *Teil. Meteor. Rundschau.* **3**, 1–7.

Kleinschmidt, E. 1950b. Uber aufbau und entstehung von zyklonen II. Teil. *Meteor. Rundschau.* **3**, 54–61.

Mason, S. J. 1995. Sea surface temperature—South African rainfall associations, 1910–1989. *Int. J. Climatol.* **15**, 119–135.

Morgan, M. C. and Neilsen-Gammon, J. W. 1998. Using tropopause maps to diagnose midlatitude weather systems. *Mon. Wea. Rev.* **126**, 2555–2579.

Palmén, E. and Newton, C. 1969. *Atmospheric circulation systems*. Academic Press, New York, 603 pp.

Reason, C. J. C. 2001. Evidence for the influence of the Agulhas Current on regional atmospheric circulation patterns. *J. Clim.* **14**, 2769–2778.

Reason, C. J. C. and Mulenga, H. M. 1999. Relationships between South African rainfall and SST anomalies in the South West Indian Ocean. *Int. J. Climatol.* **19**, 1651–1673.

Romero, R., Doswell III, C. A. and Ramis, C. 2000. Mesoscale numerical study of two cases of long-lived quasi-stationary convective systems over eastern Spain. *Mon. Wea. Rev.* **128**, 3731–3751.

Rouault, M., White, S. A., Reason, C. J. C., Lutjeharms, J. R. E. and Jobard, I. 2002. Ocean-atmosphere interaction in the Agulhas Current region and a South African extreme weather event. *Wea. Forecasting* **17**, 655–669.

Taljaard, J. J. 1985. Cut-off lows in the South African region. *South African Weather Bureau Tech. Paper* **14**, 153.

Triegaardt, D. O., Terreblanche, D. E., van Heerden, J. and Laing, M. V. 1988. The Natal floods of September 1987. *South African Weather Bureau Tech. Paper* **19**, 62.

Walker, N. D. 1990. Links between South African summer rainfall and temperature variability of the Agulhas and Benguela Current systems. *J. Geophys. Res.* **95**, 3297–3319.

Yeh, H.-C. and Chen, Y.-L. 2002. The role of offshore convergence on coastal rainfall during TAMEX IOP 3. *Mon. Wea. Rev.* **130**, 2709–2730.